

CSL *COORDINATED SCIENCE LABORATORY*

AN INVESTIGATION OF STRIP LINES AND FIN LINES WITH PERIODIC STUBS

TOSHIHIDE KITAZAWA
RAJ MITTRA

APPROVED FOR PUBLIC RELEASE. DISTRIBUTION UNLIMITED.

UNIVERSITY OF ILLINOIS AT URBANA-CHAMPAIGN

REPORT DOCUMENTATION PAGE		READ INSTRUCTIONS BEFORE COMPLETING FORM
1. REPORT NUMBER	2. GOVT ACCESSION NO.	3. RECIPIENT'S CATALOG NUMBER
4. TITLE (and Subtitle) An Investigation of Strip Lines and Fin Lines With Periodic Stubs		5. TYPE OF REPORT & PERIOD COVERED Technical Report
		6. PERFORMING ORG. REPORT NUMBER R-1002; UILU-ENG 83-2223
7. AUTHOR(s) Toshihide Kitazawa and Raj Mittra		8. CONTRACT OR GRANT NUMBER(s) N000-1479C-0424
9. PERFORMING ORGANIZATION NAME AND ADDRESS Coordinated Science Laboratory University of Illinois Urbana, IL 61801		10. PROGRAM ELEMENT, PROJECT, TASK AREA & WORK UNIT NUMBERS
11. CONTROLLING OFFICE NAME AND ADDRESS JSEP		12. REPORT DATE October 1983
		13. NUMBER OF PAGES 21
14. MONITORING AGENCY NAME & ADDRESS (if different from Controlling Office)		15. SECURITY CLASS. (of this report) Unclassified
		15a. DECLASSIFICATION/DOWNGRADING SCHEDULE
16. DISTRIBUTION STATEMENT (of this Report) Approved for public release; distribution unlimited.		
17. DISTRIBUTION STATEMENT (of the abstract entered in Block 20, if different from Report)		
18. SUPPLEMENTARY NOTES		
19. KEY WORDS (Continue on reverse side if necessary and identify by block number) fin-lines strip lines millimeter waves periodic stub filters		
20. ABSTRACT (Continue on reverse side if necessary and identify by block number) In this paper a technique based on the network analytical formalism of electro-magnetic fields is used to analyze the strip and fin lines with periodic stubs. Numerical results for the dispersion characteristics of the periodically loaded lines are presented. The effect of the loading stubs on the passband and stopband characteristics is investigated.		

AN INVESTIGATION OF STRIP LINES AND FIN LINES WITH PERIODIC STUBS

Toshihide Kitazawa* and Raj Mittra

Electrical Engineering Department
University of Illinois
Urbana, Illinois

The work reported herein was sponsored in part by the Joint Services Electronics Program, N00014-79-C-0424.

* Dr. Kitazawa is on leave from Kitami Institute of Technology, Kitami, Japan.

ABSTRACT

In this paper a technique based on the network analytical formalism of electromagnetic fields is used to analyze the strip and fin lines with periodic stubs. Numerical results for the dispersion characteristics of the periodically loaded lines are presented. The effect of the loading stubs on the passband and stopband characteristics is investigated.

I. INTRODUCTION

Propagation characteristics of planar transmission lines for microwave and millimeter-wave integrated circuits have been investigated in the past by many authors. Two of the frequently used transmission media in the microwave frequency range are the strip and slot lines while the fin-line is known to find applications in the millimeter-wave range. Hybrid-mode analyses of uniform lines of the above types [1] have been reported in the literature [2]. However, the periodic-loaded version of these lines finds useful applications in many devices, such as filters [3].

In this paper an approach for analyzing periodically loaded strip lines and fin lines is presented. The network-analytical method is employed for the formulation of an integral equation for the unknown electromagnetic fields [4] and Galerkin's procedure is used to derive a numerical solution of this equation. Numerical results present the passband and stopband properties.

II. THE NETWORK FORMULATION OF THE PROBLEM

In this section we illustrate the network-analytical method of formulation by analyzing the problem of fin lines with periodic stubs (see Fig. 1a), although the method itself is applicable to the strip-line configuration (Fig. 1b). The numerical results for both cases will be presented in the next section.

As a first step, we express the transverse (to z) fields in each region by using the Fourier transformation in the x -direction and Floquet harmonic representation in the y -direction as follows:

$$\left. \begin{array}{l} E_t^{(i)}(x, y, z) \\ H_t^{(i)}(x, y, z) \end{array} \right\} = \sum_{\ell=1}^2 \sum_{m=0}^{\infty} \sum_{n=-\infty}^{\infty} \left\{ \begin{array}{l} V_{\ell mn}^{(i)}(z) e_{\ell mn}(x, y) \\ I_{\ell mn}^{(i)}(z) h_{\ell mn}(x, y) \end{array} \right. \quad (1)$$

$i = 1, 2, 3 \text{ (regions)}$

where

$$e_{1mn}(x, y) = \sqrt{\frac{\eta_m}{2Ap}} \frac{1}{K} \{x_0 \gamma_m \cos \gamma_m(x + A) - y_0 j \beta_n \sin \gamma_m(x + A)\} e^{-j \beta_n y}$$

$$e_{2mn}(x, y) = \sqrt{\frac{\eta_m}{2Ap}} \frac{1}{K} \{x_0 j \beta_n \cos \gamma_m(x + A) - y_0 \gamma_m \sin \gamma_m(x + A)\} e^{-j \beta_n y}$$

$$h_{\ell mn}(x, y) = z_0 \times e_{\ell mn}(x, y) \quad (\ell = 1, 2)$$

$$K^2 = \gamma_m^2 + \beta_n^2, \quad \gamma_m = \frac{m\pi}{2A}, \quad \beta_n = \beta_0 + \frac{2n\pi}{p}$$

$$\eta_m = \begin{array}{ll} 1 & (m = 0) \\ 2 & (m \neq 0) \end{array} \quad \text{Neumann's number} \quad (2)$$

Here β_0 is the propagation constant of the dominant harmonic in the Floquet representation, and the vector mode functions e_{lmn} , h_{lmn} satisfy the boundary conditions at $x = \pm A$ as well as the following orthonormal properties:

$$\int_{-A}^A \int_{-P/2}^{P/2} e_{lmn}(x,y) \cdot e_{l'm'n'}^*(x,y) dx dy = \delta_{ll'} \delta_{mm'} \delta_{nn'} \quad (3)$$

where $\delta_{ll'}$ is Kronecker's delta and the symbol * signifies complex conjugate. Substituting (1) into Maxwell's field equations and applying the orthonormal properties (3), we obtain the differential equations for $V_{lmn}^{(i)}$ and $I_{lmn}^{(i)}$:

$$\begin{cases} -\frac{dV_{lmn}^{(i)}}{dz} = j \kappa_{mn}^{(i)} z_{lmn}^{(i)} I_{lmn}^{(i)} \\ -\frac{dI_{lmn}^{(i)}}{dz} = j \kappa_{mn}^{(i)} y_{lmn}^{(i)} V_{lmn}^{(i)} \end{cases} \quad (4)$$

where

$$z_{lmn}^{(i)} = \frac{\kappa_{mn}^{(i)}}{\omega \epsilon_0 \epsilon_r^{(i)}} \quad , \quad z_{2mn}^{(i)} = \frac{\omega \mu_0}{\kappa_{mn}^{(i)}}$$

$$y_{lmn}^{(i)} = \frac{1}{z_{lmn}^{(i)}} \quad , \quad \kappa_{mn}^{(i)} = \sqrt{k^2 \epsilon_r^{(i)} - K^2} \quad ,$$

$$k = \omega \sqrt{\epsilon_0 \mu_0} \quad , \quad \epsilon_r^{(i)} = \begin{cases} \epsilon_r & \text{(region (2))} \\ 1 & \text{(otherwise)} \end{cases} \quad (5)$$

The boundary conditions to be satisfied are expressed as follows:

$$V_{\ell mn}^{(1)}(d_1) = 0 \quad (6)$$

$$V_{\ell mn}^{(1)}(+0) = V_{\ell mn}^{(2)}(-0) = v_{\ell mn} \quad (7)$$

$$V_{\ell mn}^{(2)}(-d_2 + 0) = V_{\ell mn}^{(3)}(-d_2 - 0) \quad (8a)$$

$$I_{\ell mn}^{(2)}(-d_2 + 0) = I_{\ell mn}^{(3)}(-d_2 - 0) \quad (8b)$$

$$V_{\ell mn}^{(3)}(-d_2 - d_3) = 0 \quad (9)$$

and

$$H_t^{(1)}(x, y, +0) = H_t^{(2)}(x, y, -0) \quad (10)$$

(in the aperture of $z = 0$)

where

$$v_{\ell mn} = \int_{-A}^A \int_{-P/2}^{P/2} e_{\ell mn}^*(x', y') \cdot \epsilon(x', y') dx' dy' \quad (11)$$

and $\epsilon(x, y)$ is the transverse electric field in the aperture at $z = 0$.

Solution of the differential equations (4) and imposition of the boundary conditions (6) - (9) yield the unknowns $V_{\ell mn}^{(i)}$ and $I_{\ell mn}^{(i)}$ in each region. The electromagnetic fields, in turn, can be obtained by substituting $V_{\ell mn}^{(i)}$ and $I_{\ell mn}^{(i)}$ into Equation (1). Finally, applying the remaining boundary conditions (10), we may obtain the integral equation for the aperture field $\epsilon(x, y)$, and implicitly for the unknown propagation constant β_0 :

$$\sum_m \sum_n \int_{-A}^A \int_{-P/2}^{P/2} \{ Y_{1mn} h_{1mn}(x, y) e_{1mn}^*(x', y') + Y_{2mn} h_{2mn}(x, y) e_{2mn}^*(x', y') \}$$

$$\cdot \epsilon(x', y') dx' dy' = 0 \quad (12)$$

where (x,y) lies in the aperture at $z = 0$ and

$$\begin{aligned}
 Y_{1mn} = & \omega \epsilon_0 \left\{ \frac{1}{\kappa_{mn}^{(1)}} \cot (\kappa_{mn}^{(1)} d_1) \right. \\
 & \left. + \frac{\epsilon_r}{\kappa_{mn}^{(2)}} \frac{\kappa_{mn}^{(2)} - \epsilon_r \kappa_{mn}^{(3)} \tan (\kappa_{mn}^{(2)} d_2) \tan (\kappa_{mn}^{(3)} d_3)}{\kappa_{mn}^{(2)} \tan (\kappa_{mn}^{(2)} d_2) + \epsilon_r \kappa_{mn}^{(3)} \tan (\kappa_{mn}^{(3)} d_3)} \right\} \\
 Y_{2mn} = & \frac{1}{\omega \mu_0} \left\{ \kappa_{mn}^{(1)} \cot (\kappa_{mn}^{(1)} d_1) \right. \\
 & \left. + \kappa_{mn}^{(2)} \frac{\frac{1}{\kappa_{mn}^{(2)}} - \frac{1}{\kappa_{mn}^{(3)}} \tan (\kappa_{mn}^{(2)} d_2) \tan (\kappa_{mn}^{(3)} d_3)}{\frac{1}{\kappa_{mn}^{(2)}} \tan (\kappa_{mn}^{(2)} d_2) + \frac{1}{\kappa_{mn}^{(3)}} \tan (\kappa_{mn}^{(3)} d_3)} \right\} . \quad (13)
 \end{aligned}$$

The formulation is rigorous up to this stage. The numerical computation for the above equation is explained in the next section.

III. NUMERICAL COMPUTATION AND RESULTS

Equation (12) can be expressed in an operator form as

$$\bar{F}(x,y|x',y') \cdot \epsilon(x',y') = 0 \quad (14)$$

where the dyadic operator \bar{F} is given by

$$\begin{aligned} \bar{F}(x,y|x',y') \cdot = & \sum_m \sum_n \int_{-A}^A \int_{-P/2}^{P/2} \{ Y_{1mn} h_{1mn}(x,y) e_{1mn}^*(x',y') \\ & + Y_{2mn} h_{2mn}(x,y) e_{2mn}^*(x',y') \} dx' dy'. \end{aligned} \quad (15)$$

The determinantal equation for the dispersion relation can be obtained by applying Galerkin's procedure to Eq. (14). In this procedure, the unknown aperture field $\epsilon(x,y)$ is expanded in terms of the appropriate basis functions $f_k(x,y)$ as follows:

$$\epsilon(x,y) = \sum_{k=1}^N a_k f_k(x,y) \quad (16)$$

where a_k are the unknown coefficients. Substituting (16) into (14), using $f_m^*(x,y)$ as test functions and taking inner products, we obtain a set of simultaneous equations for the unknown coefficients a_k :

$$[M] [a] = 0. \quad (17a)$$

That is,

$$\begin{bmatrix} M_{11} & M_{12} & \dots & M_{1N} \\ M_{21} & & & \\ \vdots & \ddots & & \\ M_{N1} & & & M_{NN} \end{bmatrix} \begin{bmatrix} a_1 \\ a_2 \\ \vdots \\ a_N \end{bmatrix} = 0 \quad (17b)$$

where

$$M_{mk} = \int_{-A}^A \int_{-P/2}^{P/2} Z_0 \times f_m^*(x,y) \cdot \{F(x,y|x',y') \cdot f_k(x',y')\} dx dy \quad (18)$$

The determinantal equation for the propagation constant β_0 can be obtained by setting the determinant of the coefficient matrix of Eq. (17) equal to zero, i.e.,

$$\det[M(\beta_0)] = 0 \quad (19)$$

It remains only to select the basis functions $f_k(x,y)$. Before defining the basis functions, we introduce three auxiliary functions:

$$S_1(x,y) = \begin{cases} 1 & (|x| \leq W \text{ and } |y| \leq \frac{P}{2}) \\ 0 & (\text{otherwise}) \end{cases}$$

$$S_2(x,y) = \begin{cases} 1 & (|x| \leq W \text{ and } W_1 \leq |y| \leq \frac{P}{2}) \\ 0 & (\text{otherwise}) \end{cases}$$

$$S_3(x,y) = \begin{cases} 1 & (W \leq |x| \leq W + \ell \text{ and } |y| \leq W_1) \\ 0 & (\text{otherwise}) \end{cases} \quad (20)$$

The regions represented by these functions are shown in Fig. 2. The basis functions to be used are defined by employing these auxiliary functions:

$$f_1(x,y) = x_0 X(x) e^{-j\beta_0 y} S_1(x,y) \quad (21a)$$

$$f_2(x,y) = x_0 X(x) e^{-j\beta_{-1} y} S_1(x,y) \quad (21b)$$

$$f_3(x,y) = x_0 \operatorname{sgn}(y) X(x) e^{-j\beta_0 y} S_2(x,y) + y_0 \operatorname{sgn}(x) \cos \left[\frac{\pi}{2(\ell + W)} x \right] Y(y) S_3(x,y) \quad (21c)$$

$$f_4(x,y) = x_0 \operatorname{sgn}(y) X(x) e^{-j\beta_{-1}y} S_2(x,y) + y_0 \operatorname{sgn}(x) \cos \left\{ \frac{\pi}{2(\ell + W)} x \right\} Y(y) S_3(x,y) \quad (21d)$$

where

$$\beta_{-1} = \beta_0 - \frac{2\pi}{p}$$

and $X(x)$ and $Y(y)$ represent the x - and y -variations in the main- and stub-fin lines, respectively. Three different functions are used for $X(x)$ and $Y(y)$, viz.,

$$\begin{aligned} \text{i)} \quad X(x) &= \frac{C}{W}, \quad Y(y) = \frac{C}{W_1} & C: \text{ constant} \\ \text{ii)} \quad X(x) &= \frac{|x|}{W}, \quad Y(y) = \frac{|y|}{W_1} \\ \text{iii)} \quad X(x) &= \frac{1}{W} \left\{ 1 + \left| \frac{x}{W} \right|^3 \right\}, \quad Y(y) = \frac{1}{W_1} \left\{ 1 + \left| \frac{y}{W_1} \right|^3 \right\}. \end{aligned} \quad (22)$$

We mention that the functions in (21c) and (21d) are quite similar in character to the junction basis functions that have been employed in scattering problems [5].

Figure 3 shows the $k - \beta_0$ diagram for a fin line with periodic stubs. Computations have been performed for three different sets of basis functions given in (22), but the deviations were found to be rather small because Galerkin's procedure was used in the numerical computations. The curve for the periodically loaded fin line (solid line) is lower than for the uniform fin line without stubs (broken line) because of the inductive reactance of the series stubs. The passband and stopband regions, which are common in the dispersion diagrams in periodic structures [6] and are applicable to filters, are clearly

evident in Fig. 3. The first passband occurs in the frequency range when kp satisfies $1.038 < kp < 2.800$ and the first stopband $2.800 < kp < 2.931$. It should be noted that the higher-order stopbands will appear in the higher-frequency range; however, since the higher-order (even) mode of the uniform fin line (without stubs) can propagate in the range $kp > 4.315$, these higher stopbands have little significance.

Figure 4 shows the relative amplitude of the coefficients of basis functions f_1 and f_2 , which represent the $n = 0$ and $n = -1$ harmonics, respectively, at each point indicated in Fig. 3. These results show that the first stopband is caused by the coupling between the $n = 0$ and $n = -1$ harmonics.

Figure 5 shows the effect of the loading stubs on the normalized stopband width $\Delta k/k_c$, where Δk is the stopband width and k_c is the center frequency. The stub length l is smaller than the quarter wavelength of the stub fin line, so the series stubs have an inductive reactance; therefore, the longer the stub, the wider the stopband. The characteristic impedance of the fin line becomes larger as the gap becomes wider [2]; therefore, the stopband becomes wider with wider stubs, although the dependence on the stub width is relatively small.

Figure 6 shows the $k - \beta_0$ diagram of the strip line with periodic stubs. Again, the passband and stopband properties are observed in this case, with the first passband occurring when $0 < kp < 1.228$ and the first stopband when $1.228 < kp < 1.286$. The first higher-order mode of the main strip line appears when $kp = 2.289$; therefore, the higher-order stopbands have no meaning in the same way as the case of fin line.

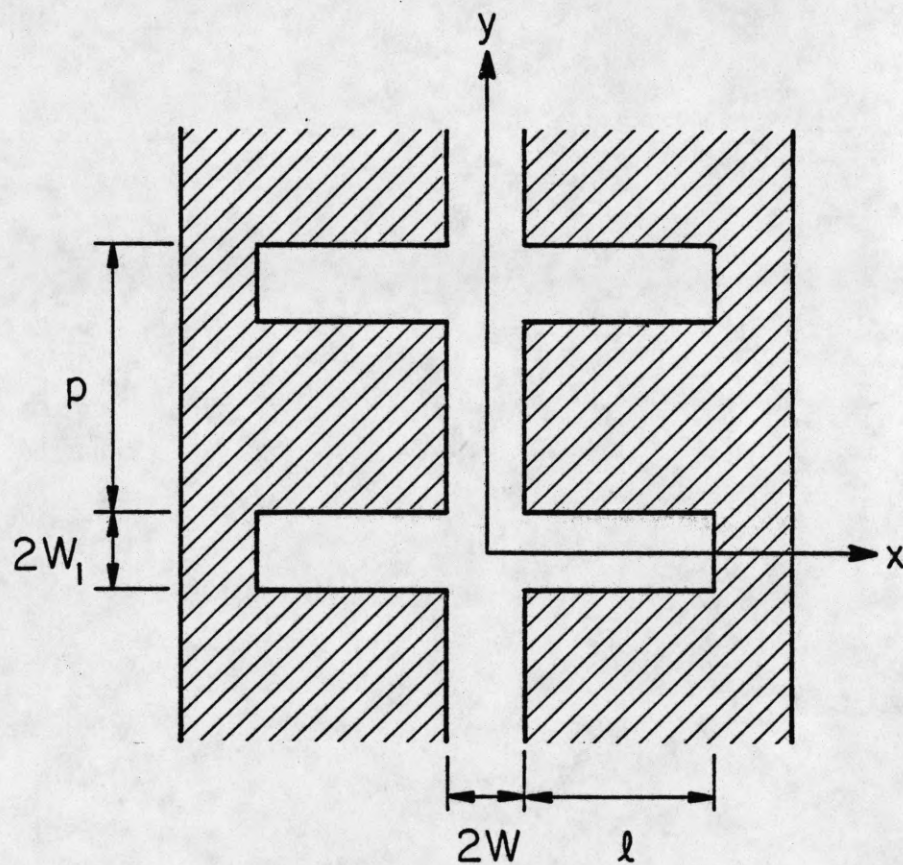
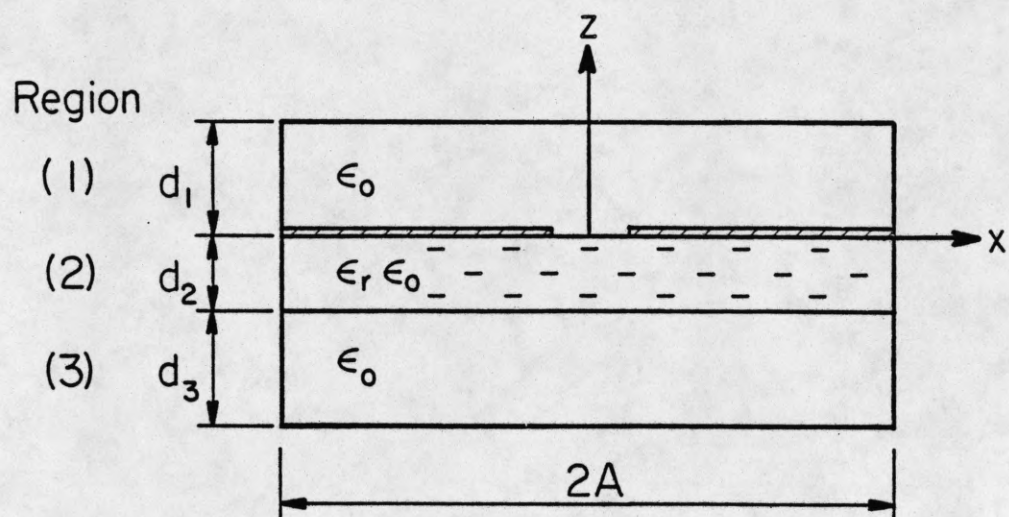
Figure 7 shows the effect of the loading stubs. The characteristic impedance of the strip line becomes smaller as the strip becomes wider [4], but the stubs are shunt-connected in this case. Therefore, the stopband, again, becomes wider with wider stubs.

IV. CONCLUSIONS

A method of analysis for the strip line and the fin line with periodic stubs has been presented, and the $k - \beta_0$ diagrams for these structures have been computed. It is found that the passband and stopband properties are generated from the coupling between the $n = 0$ and $n = -1$ harmonics. The effects of the loading stubs have been determined numerically.

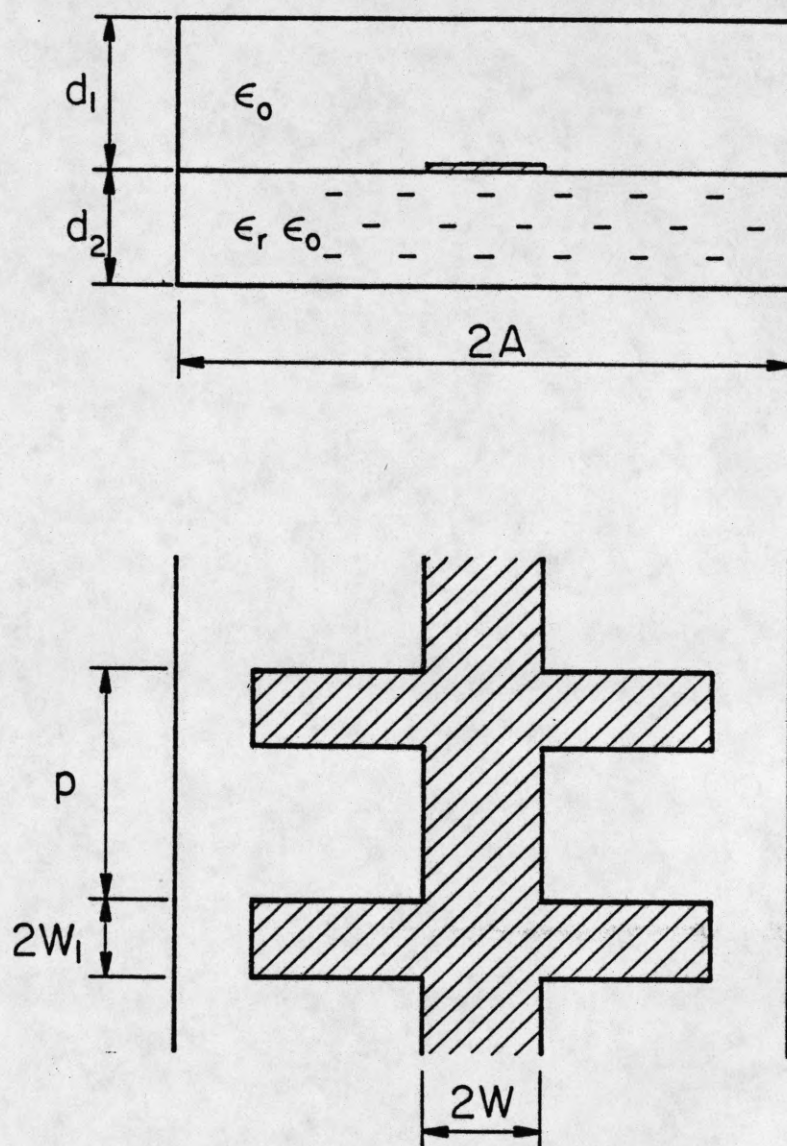
REFERENCES

- [1] G. Kowalski and R. Pregla, "Dispersion characteristics of shielded microstrips with finite thickness," Arch. Elek. Ubertragung, vol. 25, pp. 193-196, April 1971.
- [2] Y. Hayashi, E. Farr, S. Wilson, and R. Mittra, "Analysis of dominant and higher-order modes in unilateral fin lines," Arch. Elek. Ubertragung, vol. 37, pp. 117-122, March 1983.
- [3] H. Entschladen and H. J. Siweris, "Slot line stub filters," Arch. Elek. Ubertragung, vol. 34, pp. 152-156, April 1980.
- [4] T. Kitazawa and Y. Hayashi, "Propagation characteristics of strip lines with multilayered anisotropic media," IEEE Trans. Microwave Theory Tech., to be published.
- [5] C. H. Tsao and R. Mittra, "Spectral-domain analysis of frequency selective surfaces (FSS) comprised of periodic arrays of cross-dipoles and Jerusalem-crosses," to appear in IEEE Trans. Antennas Propagat.
- [6] R. E. Collin, Field Theory of Guided Waves. New York: McGraw-Hill, 1960, p. 368.



(a)

Figure 1a: Planar transmission lines with stubs - periodic-loaded fin line.



(b)

Figure 1b: Planar transmission lines with stubs - periodic-loaded strip line.

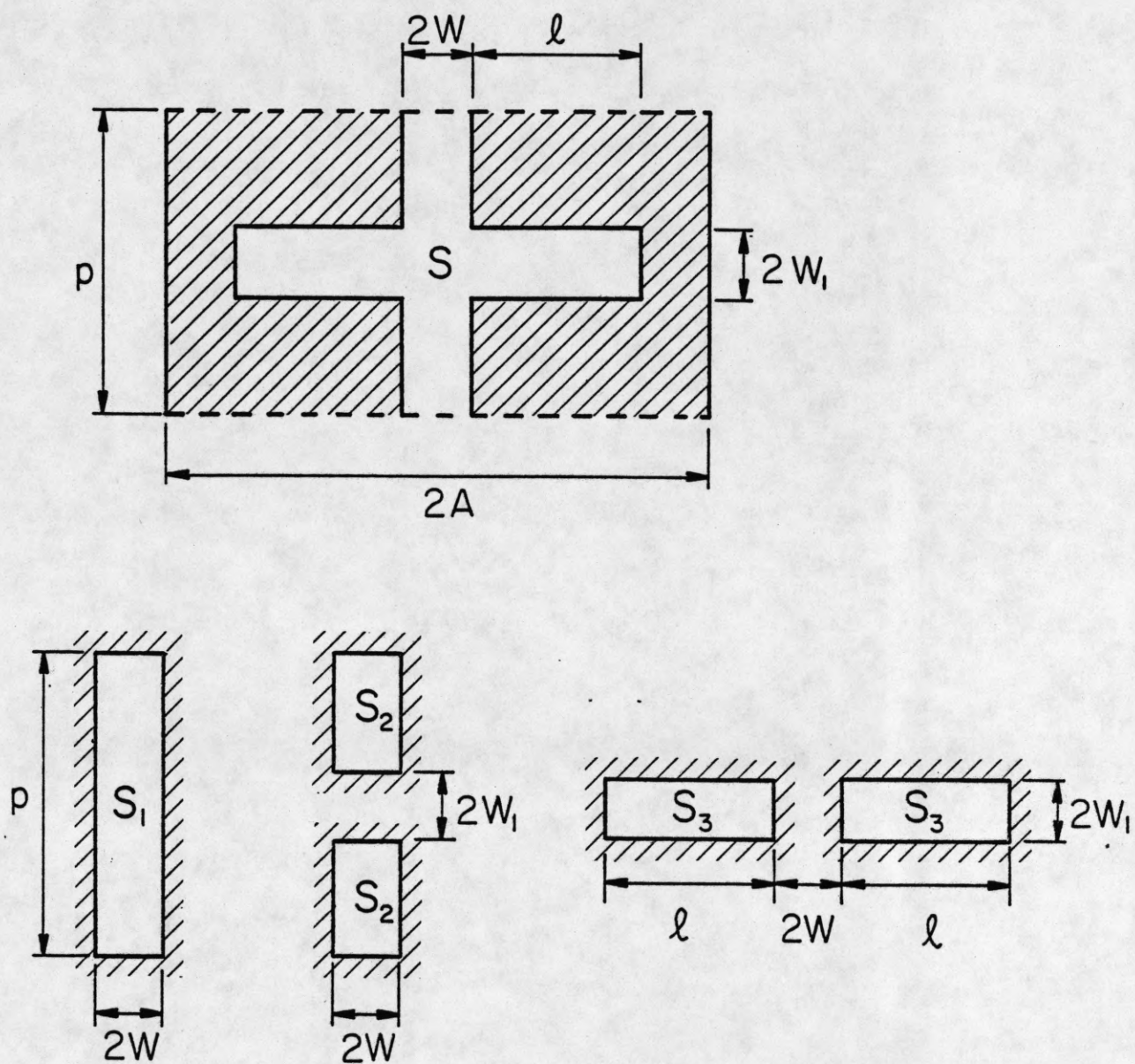


Figure 2: Regions represented by Equation (20).

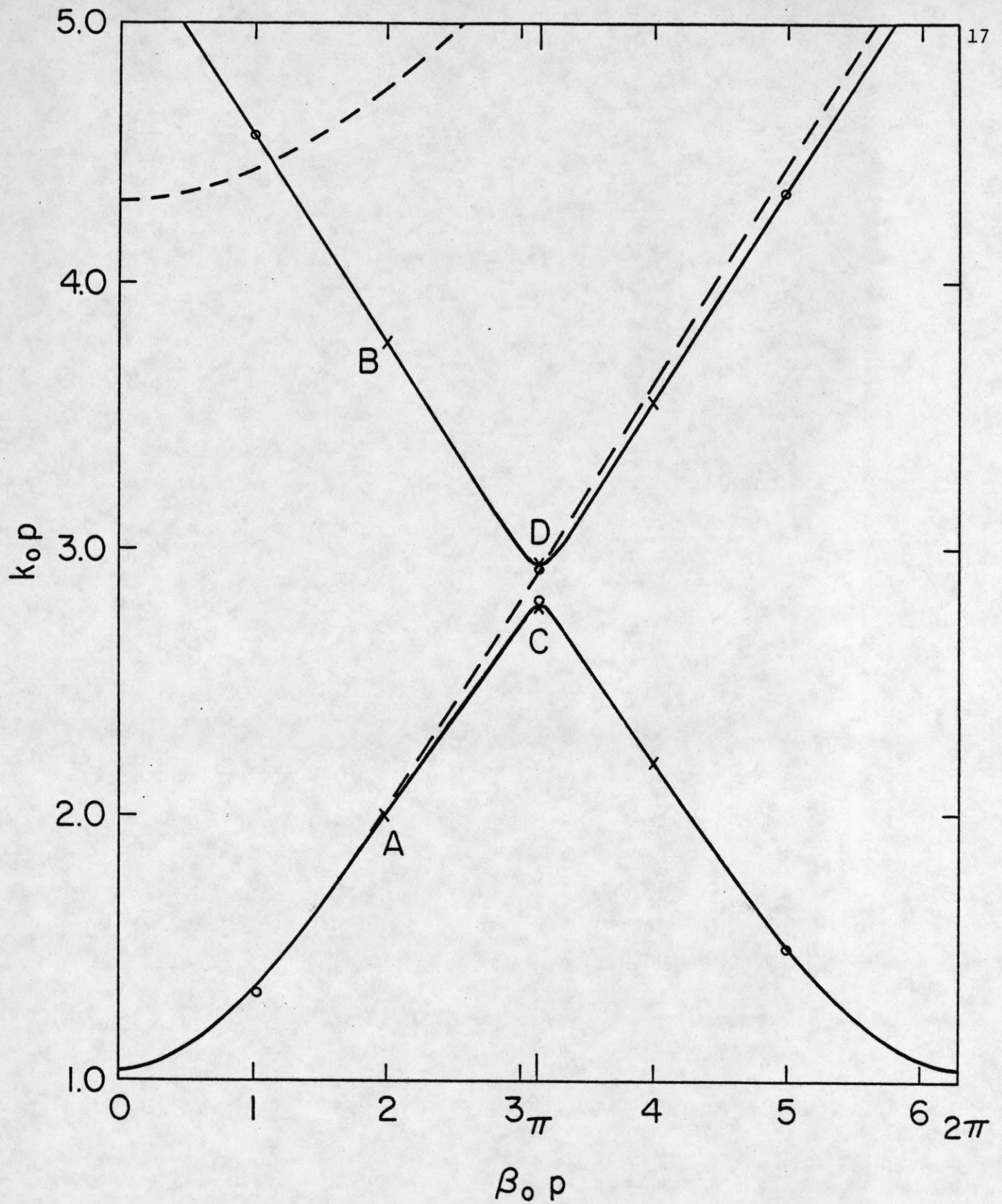
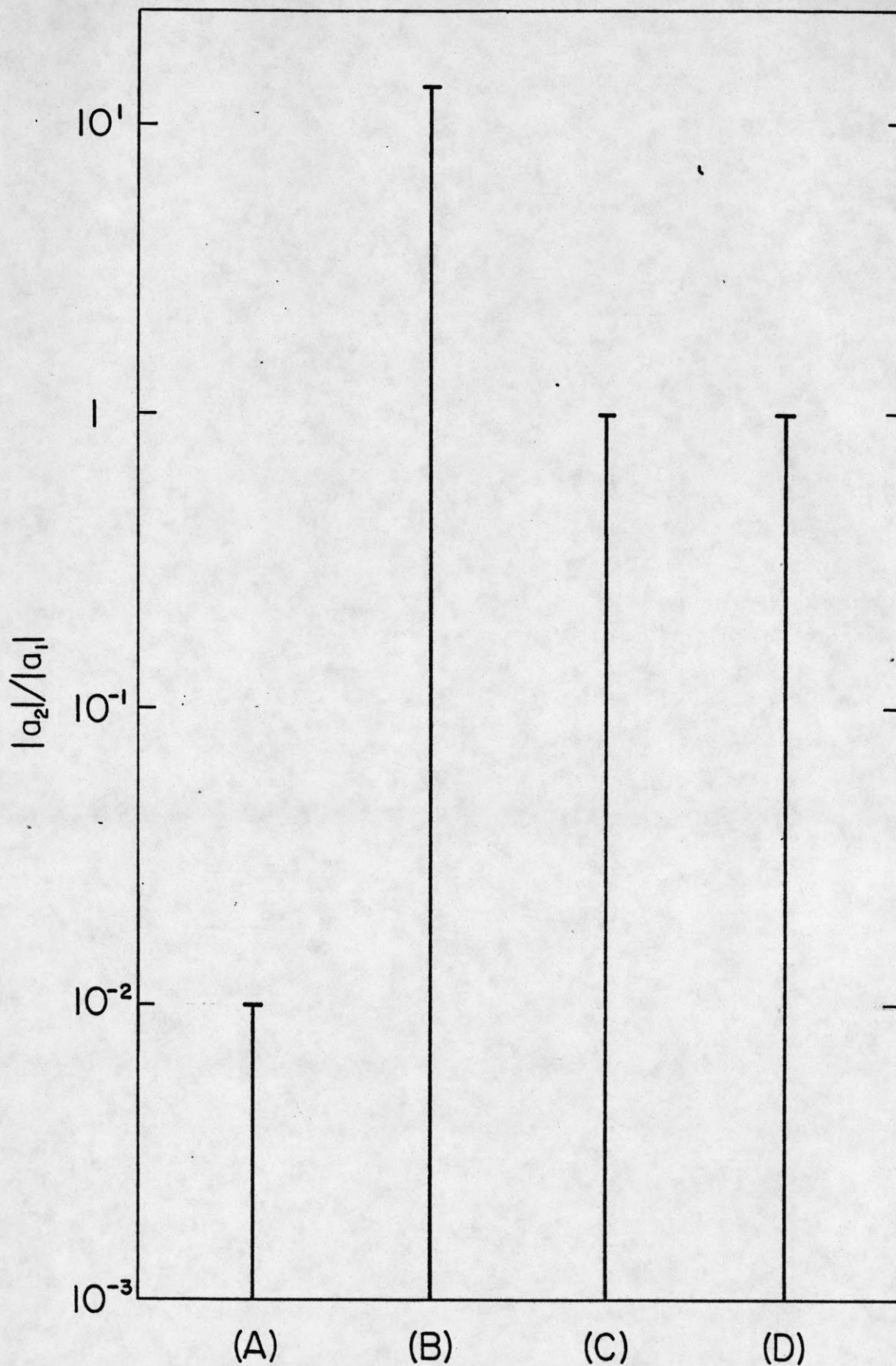


Figure 3: The $k - \beta_0$ diagram for a periodic-loaded fin line.
 $\epsilon_r = 2.2$, $d_1 = 0.094''$, $d_2 = 0.005''$, $d_3 = 0.089''$,
 $W = 0.0025''$, $A = 0.047''$, $W_1 = 0.01''$, $\ell = 0.04''$,
 $p = 0.12''$ —: fin line with stubs using iii) in
(22), ----: uniform fin line (without stubs),
O: using i) in (22), X: using ii) in (22).



Points indicated in Fig.3

Figure 4: The relative amplitude of coefficients of basis functions f_1 and f_2 .

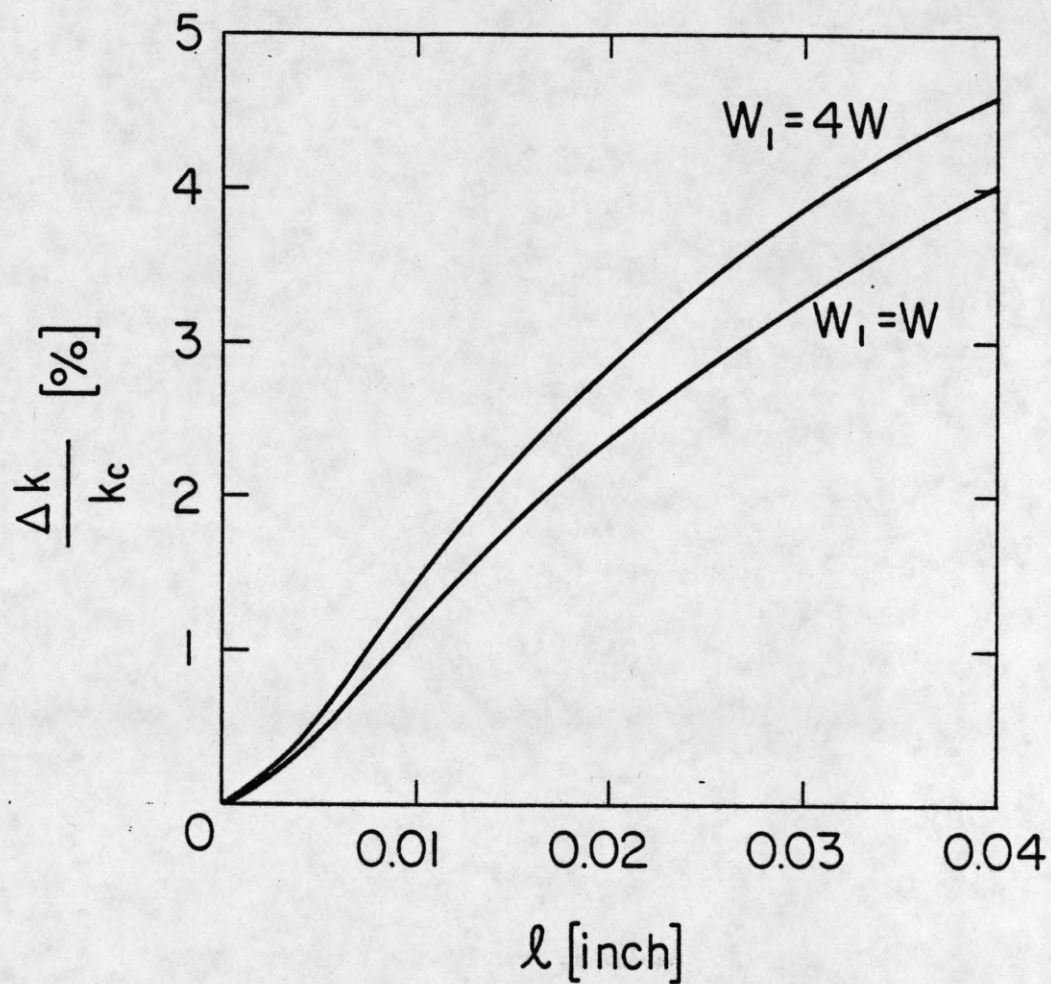


Figure 5: The effect of the loading stubs of the fin line.

$\epsilon_r = 2.2$, $d_1 = 0.094''$, $d_2 = 0.005''$, $d_3 = 0.089''$,
 $W = 0.0025''$, $A = 0.047''$, $p = 0.12''$.

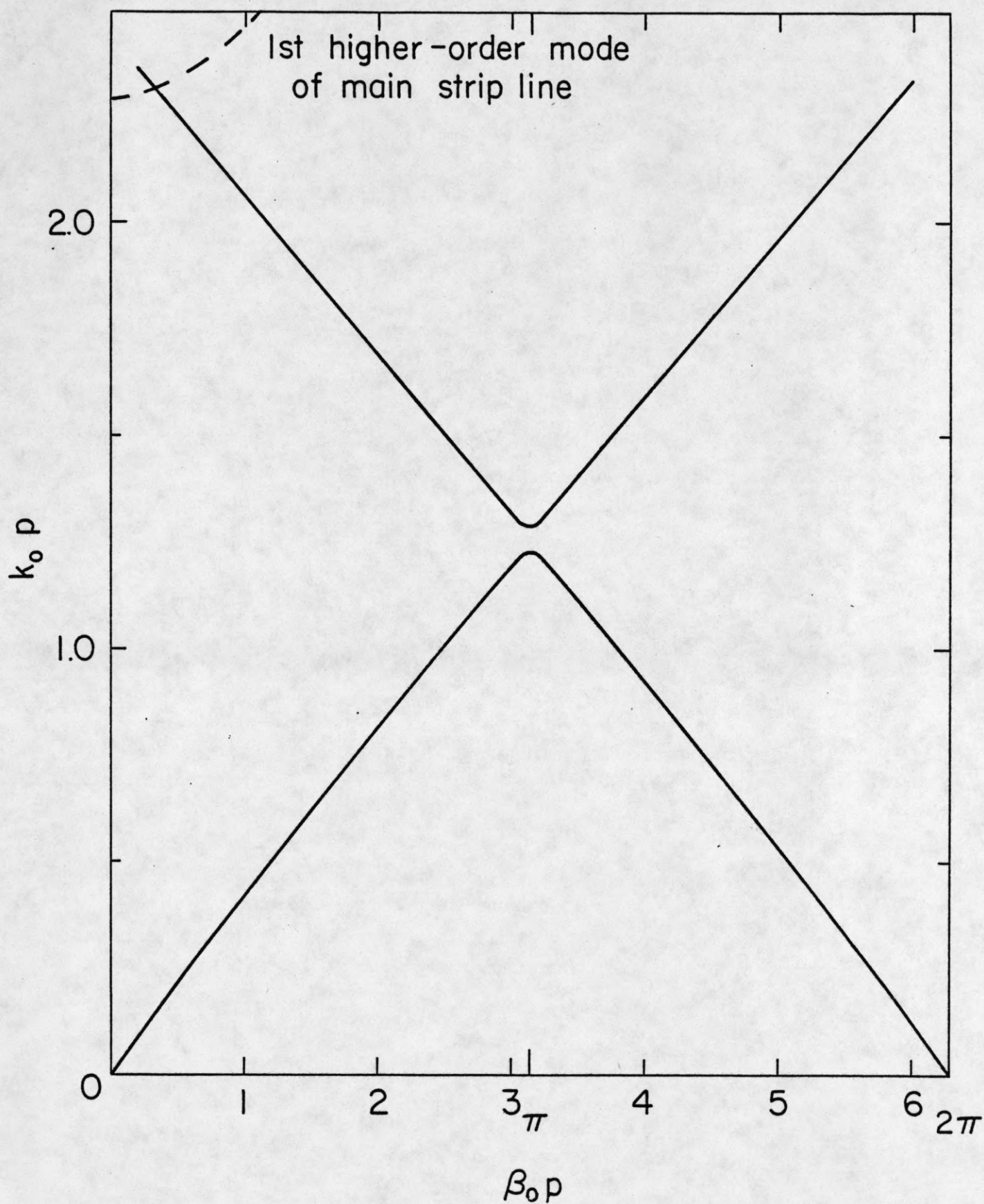


Figure 6: The $k - \beta_0$ diagram for a periodic-loaded strip line.

$\epsilon_r = 8.875$, $d_1 = 11.43(\text{mm})$, $d_2 = 1.27(\text{mm})$, $W = 0.3175(\text{mm})$,
 $A = 6.35(\text{mm})$, $W_1 = 0.3175(\text{mm})$, $l = 4(\text{mm})$, $p = 10(\text{mm})$.

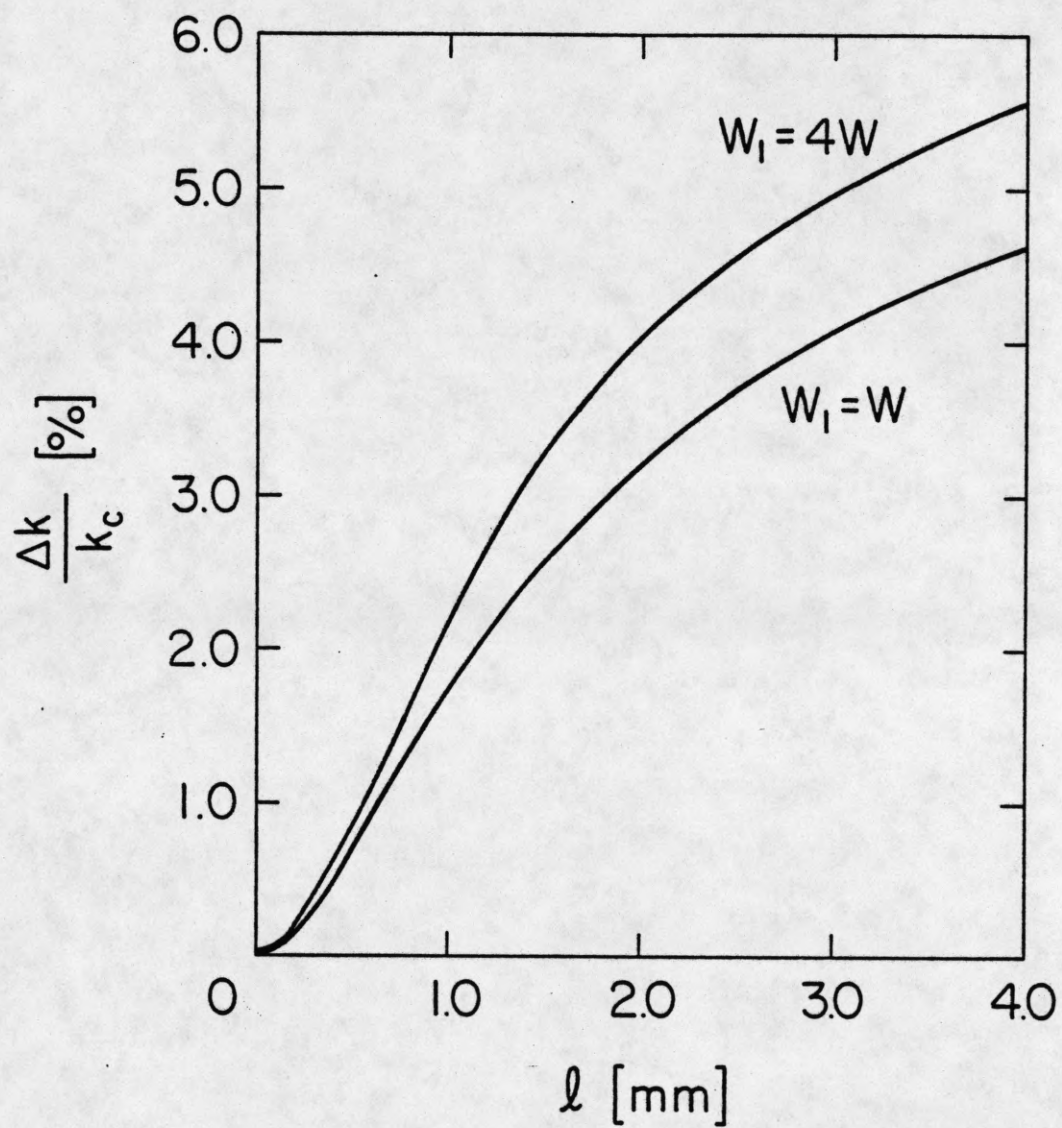


Figure 7: The effect of the loading stubs of the strip line.

$\epsilon_r = 8.875$, $d_1 = 11.43(\text{mm})$, $d_2 = 1.27(\text{mm})$, $W = 0.3175(\text{mm})$,
 $A = 6.35(\text{mm})$, $p = 10(\text{mm})$.